The Journal of Chemical Physics

Heat transport induced by electron transfer: A general temperature quantum calculation

Cite as: J. Chem. Phys. **155**, 194104 (2021); https://doi.org/10.1063/5.0068303
Submitted: 24 August 2021 • Accepted: 25 October 2021 • Accepted Manuscript Online: 27 October 2021 • Published Online: 15 November 2021

Bingyu Cui, Galen T. Craven and Abrahan Nitzan

AIP Publishing

The Journal of Chemical Physics ARTICLE scitation.org/journal/jcp

Heat transport induced by electron transfer: A general temperature quantum calculation

Cite as: J. Chem. Phys. 155, 194104 (2021); doi: 10.1063/5.0068303
Submitted: 24 August 2021 • Accepted: 25 October 2021 •
Published Online: 15 November 2021

Bingyu Cui,[1,2] Galen T. Craven,[3] and Abrahan Nitzan[1,2,a)]

AFFILIATIONS

[1] Department of Chemistry, University of Pennsylvania, Philadelphia, Pennsylvania 19104, USA
[2] School of Chemistry, Tel Aviv University, Tel Aviv 69978, Israel
[3] Theoretical Division, Los Alamos National Laboratory, Los Alamos, New Mexico 87544, USA

[a)] **Author to whom correspondence should be addressed:** anitzan@sas.upenn.edu

ABSTRACT

Electron transfer dominates chemical processes in biological, inorganic, and material chemistry. Energetic aspects of such phenomena, in particular, the energy transfer associated with the electron transfer process, have received little attention in the past but are important in designing energy conversion devices. This paper generalizes our earlier work in this direction, which was based on the semiclassical Marcus theory of electron transfer. It provides, within a simple model, a unified framework that includes the deep (nuclear) tunneling limit of electron transfer and the associated heat transfer when the donor and acceptor sites are seated in environments characterized by different local temperatures. The electron transfer induced heat conduction is shown to go through a maximum at some intermediate average temperature where quantum effects are already appreciable, and it approaches zero when the average temperature is very high (the classical limit) or very low (deep tunneling).

I. INTRODUCTION

Electron transfer (ET) processes lie at the core of oxidation–reduction reactions, ranging from photosynthesis[1] to electrochemistry,[2] corrosion,[3] and vision,[4] and are key ingredients in many subjects of present research, such as photoelectrochemistry,[5] solar energy conversion,[6] organic light-emitting diodes,[7] and molecular electronic devices.[8]

Despite its inherent limitations, Marcus theory is the most commonly used approach used for understanding such phenomena.[9,10] It relies on the timescale separation between electronic and nuclear motions and combines classical transition state theory for the nuclear motion to reach the lowest crossing point of the reactant and product nuclear potential surfaces, with the probability for elastic electron tunneling once this point is achieved. At this level of treatment, the theory cannot account for nuclear tunneling effects that become important when $\hbar\omega > k_B T$ ($2\pi/\omega$ is a typical nuclear period, T is the temperature, and k_B is the Boltzmann constant)—a common situation for intramolecular vibrations. Indeed, the Marcus expression for the electron transfer rate is the high temperature limit of a more general expression obtained by Jortner and co-workers from the golden-rule calculation of the rate,[11–14] which can also account for nuclear tunneling at low temperatures. Other techniques to address the general spin-Boson problem beyond the golden rule[15–24] will not be considered here.

An important aspect of the electron transport process is associated with energy and heat transfer,[25–38] which is manifested in the heat conductivity of metals and in a variety of thermoelectric phenomena. Nevertheless, this aspect of the dynamics is rarely addressed in molecular electron transfer processes. Two of us have addressed this problem by generalizing the standard Marcus theory of electron transfer between two molecular sites or between a molecule and a metal, to account for situations in which different sites are characterized by different local temperatures.[39,40] This generalization of Marcus theory leads to a modified expression for the electron transfer rate in terms of the different site temperatures as well as a way to calculate the heat transfer associated with the electron transfer process. In particular, it has been found that heat transfer continues to occur even when there is no net transfer of charge.[39] However, this theory is based on the same high temperature limit as Marcus theory, and it is expected to fail at low temperatures where

the nuclear dynamics associated with the electron transfer process is dominated by nuclear tunneling.

In this paper, we aim to address this deficiency by extending Jortner theory of electron transfer[11,14,41,42] to systems where the donor and acceptor sites are characterized by different temperatures, thereby generalizing the theory discussed in Ref. 39 to account for the full temperature range including the low temperature limit. Our starting point is the spin-boson Hamiltonian that describes a two-electronic-state system ($|1\rangle, |2\rangle$) coupled to a vibrational subsystem,[43]

$$\begin{aligned} \hat{H} &= \hat{H}_S + \hat{V}, \\ \hat{H}_S &= E_1|1\rangle\langle 1| + E_2|2\rangle\langle 2| + \sum_\alpha \hbar\omega_\alpha \hat{a}_\alpha^\dagger \hat{a}_\alpha \\ \hat{V} &= V_{1,2} e^{\sum_\alpha -\bar{\lambda}_\alpha(\hat{a}_\alpha^\dagger - \hat{a}_\alpha)}|1\rangle\langle 2| + V_{2,1} e^{\sum_\alpha \bar{\lambda}_\alpha(\hat{a}_\alpha^\dagger - \hat{a}_\alpha)}|2\rangle\langle 1|, \end{aligned} \tag{1}$$

where $\hat{a}_\alpha^\dagger(\hat{a}_\alpha)$ are the creation (annihilation) operator for the (assumed harmonic) vibrational normal mode α of frequency ω_α and the parameters $\bar{\lambda}_\alpha$ account for the coupling of the boson field to the electronic transition. Equation (1) represents the standard shifted harmonic approximation that the vibronic coupling is expressed by the fact that the equilibrium positions associated with the vibrational normal modes are shifted between the two electronic states. The dimensionless shifts $\bar{\lambda}_\alpha$ are related to shifts of dimensioned coordinates λ_α and the oscillator mass m_α by

$$\bar{\lambda}_\alpha \equiv \lambda^\alpha \sqrt{\frac{m_\alpha \omega_\alpha}{2\hbar}} \tag{2}$$

and to the reorganization energy by

$$E_r = \sum_\alpha \bar{\lambda}_\alpha^2 \hbar\omega_\alpha. \tag{3}$$

In the present application, following Ref. 39, we envision electronic states 1 and 2 as describing situations where an excess electron is localized near sites a and b that are spatially separated and characterized by different local temperatures T_a and T_b, respectively. In Marcus theory and its extensions, these local temperatures are properties of the nuclear environments: we assume that the vibrational modes that couple to this transition can be divided into two groups that are localized near sites a and b and respond to their electronic populations as well as their local temperatures. As in the Marcus, Hush, Levich and Jortner versions of the theory, we assume that the thermal relaxation of the nuclear oscillations is fast relative to the electron transfer process, so these two groups of oscillators are assumed to be at equilibrium with their local temperatures.

The case $T_a = T_b \equiv T$ corresponds to the standard theory of electron transfer. The golden rule expression for the thermally averaged electron transfer rate is given in terms of the so-called generating function $G(\omega)$ by[43]

$$k_{1\to 2} = \frac{|V_{12}|^2}{\hbar^2} \tilde{G}(\omega_{12}), \tag{4}$$

where

$$\tilde{G}(\omega) = \int_{-\infty}^{\infty} dt e^{i\omega t} G(t) \tag{5}$$

and

$$G(t) = e^{-\sum_\alpha \bar{\lambda}_\alpha^2 (2n_\alpha(T)+1) + \sum_\alpha \bar{\lambda}_\alpha^2 (n_\alpha(T) e^{i\omega_\alpha t} + (n_\alpha(T)+1) e^{-i\omega_\alpha t})}. \tag{6}$$

In Eqs. (2)–(4), $\hbar\omega_{12} \equiv E_1 - E_2$ is the energy difference between electronic energy origins of the respective states, V_{12} is the electron tunneling matrix element, and

$$n_\alpha(T) = \frac{1}{\exp(\hbar\omega_\alpha/k_B T) - 1} \tag{7}$$

is the average phonon population. In the high temperature/strong coupling limit where $\bar{\lambda}_\alpha n_\alpha \gg 1$ for all α, the integral (5) can be evaluated in the short time approximation, $\exp[\pm i\omega_\alpha t] \approx 1 \pm i\omega_\alpha t - \omega_\alpha^2 t^2/2$, leading to

$$\tilde{G}(\omega) \approx \sqrt{\frac{2\pi}{2D}} e^{-\frac{(\omega - E_r/\hbar)^2}{4D}}, \tag{8}$$

where $D = \sum_\alpha (2n_\alpha(T) + 1)\bar{\lambda}_\alpha^2 \omega_\alpha^2/2$. Using $2n_{\alpha(T)} + 1 \approx 2k_B T/\omega_\alpha$, together with Eq. (4), yields the Marcus expression for the electron rate,[9,10]

$$k_{1\to 2} = \frac{|V_{12}|^2}{\hbar} \sqrt{\frac{\pi}{E_r k_B T}} \exp\left[-\frac{(E_{12} - E_r)^2}{4E_r k_B T}\right]. \tag{9}$$

Note that Eqs. (5) and (8) satisfy the identity

$$e^{\beta\hbar\omega} \tilde{G}(-\omega) = \tilde{G}(\omega); \beta = (k_B T)^{-1}, \tag{10}$$

implying that this rate expression satisfies the detailed balance relation,

$$k_{1\to 2} = k_{2\to 1} \exp[\beta(E_1 - E_2)]. \tag{11}$$

As mentioned above, this result has been generalized in Ref. 39 to account for the different site temperatures, $T_a \neq T_b$, leading also to an expression for the amount of heat transferred per electron transfer event. Here, we present a similar calculation based on Eqs. (2)–(4) without resorting to the high temperature limit. The generalized expression for the electron transfer rate is derived in Sec. II, and in Sec. III, we examine the implications associated with the energy (heat) transfer rate, making it possible to examine its phenomenon in the full temperature range including $T \to 0$. Section IV summarizes our findings.

II. THE GOLDEN RULE TRANSITION RATE IN A BITHERMAL SYSTEM

As outlined above, generalizing the electron transfer rate expression to the multi-thermal case is done by assigning different temperatures to different vibrational modes, assuming that such a group represents modes that are localized near sites with different local temperatures. Focusing on the bithermal case, the fact that the function $G(t)$ is a product over terms defined for individual modes makes it possible to write the corresponding function in the form

$$G(t) = G_a(t) G_b(t), \tag{12}$$

where

$$G_j(t) = e^{\sum_{\alpha\in j}\left[-\tilde{\lambda}_\alpha^2(2n_{j\alpha}+1)+\tilde{\lambda}_\alpha^2(n_{j\alpha}e^{i\omega_\alpha t}+(n_{j\alpha}+1)e^{-i\omega_\alpha t})\right]},$$
$$n_{j\alpha} = n_\alpha(T_j), \quad j = a, b. \tag{13}$$

Using Eqs. (2)–(4), this leads to

$$k_{1\to 2} = \frac{|V_{12}|^2}{\hbar^2}\int_{-\infty}^{\infty} d\omega \tilde{G}_a(\omega)\tilde{G}_b(\omega_{12}-\omega). \tag{14}$$

In the high temperature limit, we use Eq. (8) in Eq. (14) to get[39]

$$k_{1\to 2} \propto \sqrt{\frac{1}{T_a E_{r_a} + T_b E_{r_b}}}\exp\left[-\frac{(E_{12}+E_{r_a}+E_{r_b})^2}{4(T_a E_{r_a}+T_b E_{r_b})}\right], \tag{15}$$

where E_{r_j}, $j = a, b$ are the reorganization energies associated with the a and b mode groups that are localized at sites a and b of local temperatures T_a and T_b, respectively. To account for the full temperature range, the functions $\tilde{G}(\omega)$ need to be evaluated without invoking this high T approximation. These are well defined only when the set of vibrational modes contributing to the generating functions G constitute a continuous manifold, or after suitable broadening of the vibrational levels is introduced to account for the relaxation processes that keep the molecular sites a and b in equilibrium with their local environments (see Chapter 12 in Ref. 43). However, insight can be gained by considering continuous approximation to the function $\tilde{G}(\omega)$ even at simpler cases. For the case of a single vibrational mode ω_0 with corresponding coupling and population defined as $\tilde{\lambda}_0$ and n_0, respectively, Eqs. (5) and (6) lead to

$$\tilde{G}(\omega) = e^{-\tilde{\lambda}_0^2(2n_0+1)}\int_{-\infty}^{\infty} dt e^{i\omega t}\sum_{m,n}^{\infty}\frac{\tilde{\lambda}_0^{2(m+n)}(n_0)^m(n_0+1)^n e^{im\omega_0 t - in\omega_0 t}}{m!n!}. \tag{16}$$

The true integrals yield Dirac δ-functions for $\omega = l\omega_0$ (l integer). Replacing these according to $\delta(\omega - l\omega_0) = \delta_{\omega,l\omega_0}/\omega_0$ (effectively broadening the Dirac δ-functions) and using the Γ function to represent factorials $m! = \Gamma(m+1)$ lead to

$$\tilde{G}(\omega) = 2\pi e^{-\tilde{\lambda}_0^2(2n_0+1)}\sum_{p=0}^{\infty}\frac{\tilde{\lambda}_0^{4p} n_0^p (n_0+1)^p}{\omega_0 p!}\frac{\tilde{\lambda}_0^{\frac{2\omega}{\omega_0}}(n_0+1)^{\frac{\omega}{\omega_0}}}{\Gamma(p+\omega/\omega_0+1)}H\left(\frac{\omega}{\omega_0}+p\right), \tag{17}$$

where $H(x) = 1, x \geq 0; H(x) = 0, x < 0$ is the Heaviside function. Similar expressions for many modes are provided in the supplementary material (Sec. I). It is important to note that any approximation used for this calculation that does not satisfy the detailed balance condition, Eq. (10), may lead to artifacts, in particular, to heat transfer that does not vanish in the limit $T_a = T_b$. In the supplementary material (Sec. II), we show that these approximate expressions for $\tilde{G}(\omega)$ satisfy the detailed balance condition, Eq. (10).

Figure 1 compares a calculation based on Eq. (17) to the high temperature approximation, Eq. (8). For convenience, in all figures, we have set $k_B = \hbar = 1$ and use ω_0 and ω_0^{-1} as energy and time units, respectively. Clearly, the results coincide when T is large, as expected.

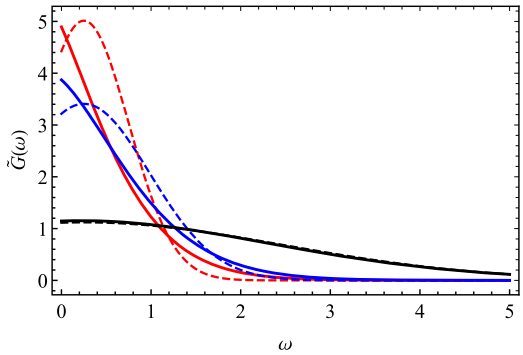

FIG. 1. A comparison between Eq. (8) (high temperature approximation, dashed lines) and Eq. (17) (general temperature expression, solid lines) at different temperatures: $T = 0.1$ (red), 1 (blue), and 10 (black), $\tilde{\lambda}_0 = 0.5$, and $\omega_0 = 1$.

To conclude this section, we note that in the high T limit, it was shown in Ref. 39 that a consequence of this model is the absence of a thermoelectric effect in the sense that if sites a and b are identical (which implies that $E_1 = E_2$ and that a similar set of local modes are associated with each site), consequently, $k_{1\to 2} = k_{2\to 1}$ even when their local temperatures are different, $T_a \neq T_b$. It is easily realized that, with $\omega_{12} = 0$, the same conclusion is reached from the more general Eq. (14).

III. HEAT TRANSFER

Next, we address the energy transfer associated with the electron transfer process. Consider first a single $1 \to 2$ process, namely, electron going from site a to site b, releasing an amount of electronic energy $\hbar\omega_{12}$ into these environment. The rate expression [Eq. (14)] is an integral over all ω of product $\tilde{G}_a(\omega_{12}-\omega)\tilde{G}_b(\omega)$, in which arguments ω and $\omega_{12}-\omega$ correspond to the amount of energy deposited into (if the corresponding argument is positive) or taken from (if negative) the corresponding groups (a and b, respectively) of vibrational modes. The sum of these arguments, ω_{12}, is the net energy transferred from the electronic to the nuclear degrees of freedom, while ω represents an amount of energy transferred from (if positive) group a to group b of vibrational modes.[44] Consequently, the probability density that for a single $1 \to 2$ event the energy change in the environment of site b is $\hbar\omega$ [and in site a is $\hbar(\omega_{12}-\omega)$] is given by

$$P_b^{1\to 2}(\omega) = \frac{\tilde{G}_a(\omega_{12}-\omega)\tilde{G}_b(\omega)}{\int_{-\infty}^{\infty} d\omega \tilde{G}_a(\omega_{12}-\omega)\tilde{G}_b(\omega)}. \tag{18a}$$

Similarly, the probability density that the energy changes near a and b per one $2 \to 1$ event are $\hbar(\omega_{21}-\omega)$ and $\hbar\omega$, respectively, is

$$P_b^{2\to 1}(\omega) = \frac{\tilde{G}_a(\omega_{21}-\omega)\tilde{G}_b(\omega)}{\int_{-\infty}^{\infty} d\omega \tilde{G}_a(\omega_{21}-\omega)\tilde{G}_b(\omega)}. \tag{18b}$$

Obviously, we can also use equivalent forms of these equations for the probability that an amount of energy $\hbar\omega$ is deposited at a site,

$$P_a^{1\to 2}(\omega) = \frac{\tilde{G}_a(\omega)\tilde{G}_b(\omega_{12}-\omega)}{\int_{-\infty}^{\infty} d\omega \tilde{G}_a(\omega)\tilde{G}_b(\omega_{12}-\omega)}, \tag{19a}$$

$$P_a^{2\to 1}(\omega) = \frac{\tilde{G}_a(\omega)\tilde{G}_b(\omega_{21}-\omega)}{\int_{-\infty}^{\infty} d\omega \tilde{G}_a(\omega)\tilde{G}_b(\omega_{21}-\omega)}. \tag{19b}$$

The average energy transferred from a to b (when positive) or b to a (when negative) per round trip $1 \to 2 \to 1$ (electron goes from site a to b and then back from b to a) is

$$\begin{aligned} Q_{a\to b}^{1\to 2\to 1} &= Q_{a\to b}^{2\to 1\to 2} = Q_b^{1\to 2} + Q_b^{2\to 1} \\ &= \hbar \int_{-\infty}^{\infty} d\omega \omega \left(P_b^{1\to 2}(\omega) + (P_b^{2\to 1}(\omega)\right) \\ &= -(Q_a^{1\to 2} + Q_a^{2\to 1}) \\ &= -Q_{b\to a}^{1\to 2\to 1}, \end{aligned} \tag{20}$$

where

$$Q_j^{1\to 2} = \hbar \int_{-\infty}^{\infty} d\omega \omega P_j^{1\to 2}(\omega), j = a, b. \tag{21}$$

Two comments are in order concerning these results. First, using the detailed balance equation, it is easy to obtain identities such as

$$\begin{aligned} &\frac{\int_{-\infty}^{\infty} d\omega \omega \tilde{G}_a(\omega_{21}-\omega)\tilde{G}_b(\omega)}{\int_{-\infty}^{\infty} d\omega \tilde{G}_a(\omega_{21}-\omega)\tilde{G}_b(\omega)} \\ &\quad = -\frac{\int_{-\infty}^{\infty} d\omega e^{-\beta_{ab}\hbar\omega} \omega \tilde{G}_a(\omega_{12}-\omega)\tilde{G}_b(\omega)}{\int_{-\infty}^{\infty} d\omega e^{-\beta_{ab}\hbar\omega} \tilde{G}_a(\omega_{12}-\omega)\tilde{G}_b(\omega)}, \end{aligned} \tag{22}$$

where $\beta_{ab} = \beta_a - \beta_b$ and $\beta_j = (k_B T_j)^{-1}, j = a, b$. Equations (20)–(22) lead to

$$\begin{aligned} Q_{a\to b}^{1\to 2\to 1} = &\frac{\int_{-\infty}^{\infty} d\omega \omega \tilde{G}_a(\omega_{12}-\omega)\tilde{G}_b(\omega)}{\int_{-\infty}^{\infty} d\omega \tilde{G}_a(\omega_{12}-\omega)\tilde{G}_b(\omega)} \\ &- \frac{\int_{-\infty}^{\infty} d\omega e^{-\beta_{ab}\hbar\omega} \omega \tilde{G}_a(\omega_{12}-\omega)\tilde{G}_b(\omega)}{\int_{-\infty}^{\infty} d\omega e^{-\beta_{ab}\hbar\omega} \tilde{G}_a(\omega_{12}-\omega)\tilde{G}_b(\omega)}, \end{aligned} \tag{23}$$

which can be shown (in the supplementary material, Sec. III) to be negative if $\beta_a > \beta_b$, implying that heat is transferred from the hotter to colder site, as expected.

Second, as defined, the single event quantities $Q_b^{1\to 2}$ and $Q_b^{2\to 1}$ represent the average energy change at site b associated with the corresponding events, but do not represent net energy transfer from a to b because they contain also the energy exchange between the electronic and vibrational subsystems. However, the contribution of the latter cancels in the round trip quantity, Eq. (20), so that $Q_{a\to b}^{1\to 2\to 1}$ represents the actual heat transferred from a to b (if positive), which is associated with such an event sequence. If we keep the two sites at different temperatures T_a and T_b, the system will reach at long time an electronic quasi-equilibrium, in which $k_{1\to 2}P_1 = k_{2\to 1}P_2$, where $P_j, (j = 1, 2)$ is the probability that the system is in state j. In this electronic quasi-equilibrium, $k_{1\to 2}P_1 = k_{2\to 1}P_2$ is the number of round trips per unit time, so the heat current (energy transferred per unit time) is

$$J = k_{1\to 2} P_1 Q_{a\to b}^{1\to 2\to 1}. \tag{24}$$

A. The high temperature limit

In this limit, the functions $G_j(\omega)$ are given by Eq. (8), namely,

$$\tilde{G}_j(\omega) \approx \sqrt{\frac{2\pi}{2k_B T_j E_{r_j}}} e^{-\frac{(\omega - E_{r_j}/\hbar)^2}{4k_B T_j E_{r_j}}}. \tag{25}$$

Using Eq. (25) in Eq. (20) leads to

$$\begin{aligned} Q_a^{1\to 2} &= \frac{(T_b - T_a)E_{r_a}E_{r_b} + T_a E_{r_a}\omega_{12}}{T_a E_{r_a} + T_b E_{r_b}}, \\ Q_a^{2\to 1} &= \frac{(T_b - T_a)E_{r_a}E_{r_b} + T_b E_{r_b}\omega_{21}}{T_a E_{r_a} + T_b E_{r_b}}, \end{aligned} \tag{26a}$$

$$\begin{aligned} Q_b^{1\to 2} &= \frac{(T_a - T_b)E_{r_a}E_{r_b} + T_b E_{r_b}\omega_{12}}{T_a E_{r_a} + T_b E_{r_b}}, \\ Q_b^{2\to 1} &= \frac{(T_a - T_b)E_{r_a}E_{r_b} + T_a E_{r_a}\omega_{21}}{T_a E_{r_a} + T_b E_{r_b}}, \end{aligned} \tag{26b}$$

and

$$Q_{b\to a}^{1\to 2\to 1} = -Q_{a\to b}^{1\to 2\to 1} = \frac{2E_{r_a}E_{r_b}(T_b - T_a)}{T_a E_{r_a} + T_b E_{r_b}}. \tag{27}$$

These results are identical to those obtained in the same high-temperature limit using a different approach.[39] Finally, the heat conduction coefficient may be defined as the factor multiplying the energy difference $T_b - T_a$ in the heat current expression obtained from Eqs. (24) and (27),

$$\sigma = \frac{2E_{r_a}E_{r_b}k_{1\to 2}P_a}{T_a E_{r_a} + T_b E_{r_b}}. \tag{28}$$

It is interesting to note that the heat transfer in the high T limit is independent of the energy gap, E_{12}, between two electronic states associated with electron localization at sites a and b.

B. The general temperature case

In what follows, we focus on a particularly simple model, aiming to elucidate the characteristic behavior of electron transfer induced heat transfer as the average temperature decreases. To this end, we use a model with just two vibrational modes, one of frequency ω_a localized at the a site at equilibrium with the local temperature T_a and the other of frequency ω_b localized at the site b at temperature T_b. A closed, although cumbersome, analytical expression can be obtained when $\omega_a = \omega_b \equiv \omega_0$ [and can provide a good approximation using $\omega_0 = (\omega_a + \omega_b)/2$ when $\omega_a \approx \omega_b$] using a procedure based on Eq. (17). It leads to (for details, see the supplementary material, Sec. IV)

$$Q_{b\to a}^{1\to 2\to 1} = \frac{Q_U(T_a,T_b,\omega_{12})}{Q_B(T_a,T_b,\omega_{12})} + \frac{Q_U(T_a,T_b,\omega_{21})}{Q_B(T_a,T_b,\omega_{21})},$$

$$Q_U(T_a,T_b,\omega_{12}) = \hbar\sum_{q=0}^{\infty}\frac{[\bar\lambda_\alpha^2 n_\alpha(T_a)+\bar\lambda_\beta^2 n_\beta(T_b)]^q}{q!}H\left(q-\frac{\omega_{12}}{\omega_0}\right) \tag{29a}$$

$$\times\left\{\frac{\bar\lambda_\alpha^2\bar\lambda_\beta^2(n_\beta(T_b)-n_\alpha(T_a))L(T_a,T_b,\omega_{12})}{q-\frac{\omega_{12}}{\omega_0}+1} - \frac{\omega_{12}\bar\lambda_\alpha^2(n_\alpha(T_a)+1)L(T_a,T_b,\omega_{12})}{\omega_0[\bar\lambda_\alpha^2(n_\alpha(T_a)+1)+\bar\lambda_\beta^2(n_\beta(T_b)+1)]}\right\}, \tag{29b}$$

$$Q_B(T_a,T_b,\omega_{12}) = \sum_{q=0}^{\infty}\frac{[\bar\lambda_\alpha^2 n_\alpha(T_a)+\bar\lambda_\beta^2 n_\beta(T_b)]^q}{\omega_0 q!} \times L(T_a,T_b,\omega_{12})H\left(q-\frac{\omega_{12}}{\omega_0}\right), \tag{29c}$$

$$L(T_a,T_b,\omega_{12}) = \frac{[\bar\lambda_\alpha^2(n_\alpha(T_a)+1)+\bar\lambda_\beta^2(n_\beta(T_b)+1)]^{q-\frac{\omega_{12}}{\omega_0}}}{\Gamma\left(q-\frac{\omega_{12}}{\omega_0}+1\right)}. \tag{29d}$$

Note that, to account for energy conservation, the frequency gap between two sites ω_{12} must be chosen to be an integer multiple of ω_0.

Figure 2 shows the heat transfer per round-trip, $Q_{b\to a}^{1\to 2\to 1}$, as a function of temperature T_b at the b site, for a given temperature at the a site: $T_a = 0.2$ and $T_a = 20$ in panels (a) and (b), respectively, comparing the results of Eq. (27) (dashed line) and (29) (solid lines) for two values of ω_{12}. In the high temperature regime, the two calculations agree and the calculated heat transfer does not depend on ω_{12}. The vanishing of the net heat transfer at $T_a = T_b$, seen at both the low and high T panels, is a sensitive test of the robustness of our approximations.

Figures 3 and 4 provide different views of the ratio $Q_{b\to a}^{1\to 2\to 1}/\Delta T$ ($\Delta T = T_b - T_a$ is the temperature difference between two sites) plotted against $T_{AV} = (T_a + T_b)/2$, keeping $\Delta T = 0.02$ throughout. For this small value of ΔT, this ratio does not depend explicitly on ΔT and may be identified as a temperature dependent heat conduction provided that $\Delta T \ll T_{AV}$. In Fig. 3, we compare the exact result and the high T approximation for the symmetric case of identical sites, $\hbar\omega_{12} = 0$, for two different values of the reorganization energy, $E_{ra} = E_{rb} = 0.3$ and 1.0. Figure 4 shows similar results, comparing the cases $\hbar\omega_{12} = 0$ and $\hbar\omega_{12} = 3$ for the same values of the reorganization energies.

Finally, in Fig. 5, we show the dependence of the heat transfer, Eq. (23), and current, Eq. (24), on the site reorganization energy (for simplicity, we consider two identical sites). Note that when the sites are identical, the probability that the system is in either state of 1 or 2 is 1/2. Panel (a) shows the heat transfer per round-trip process, $Q_{b\to a}^{1\to 2\to 1}/\Delta T$, indicating a monotonous increase in heat transfer with reorganization energy, consistent with Figs. 3 and 4. Panel (b) shows the heat flux, Eq. (24), yielding a non-monotonous behavior (which persists also in the high T limit): the heat flux vanishes (as the electron rate does) when $E_r \to 0$ and $E_r \to \infty$, and goes though a maximum in between, reflecting the behavior of the electron transfer rate in these limits.

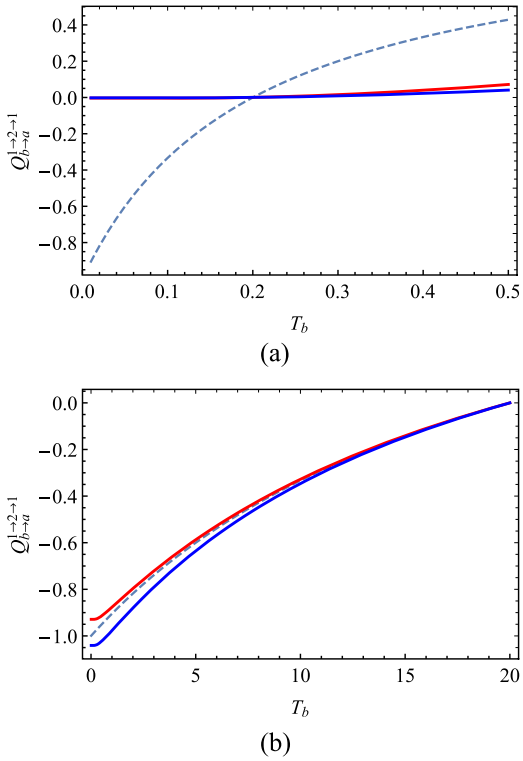

FIG. 2. The heat transfer into site a over a round process, $Q_{b\to a}^{1\to 2\to 1}$, as a function of temperature T_b, calculated by Eq. (27) (high temperature approximation, dashed lines), together with the general T results, i.e., Eq. (29) (general temperature, solid lines). Parameters are $E_{r_a} = E_{r_b} = 0.5$. Panel (a) shows $\omega_{12} = 0$ (red) and 10 (blue) results at $T_a = 0.2$. Panel (b) compares $\omega_{12} = 0$ and $\omega_{12} = 10$ in the $T_a = 20$ case. All parameters are units of $\omega_a = \omega_b \equiv \omega_0$.

The following observations can be made:

(a) The present calculation, which generalizes our earlier Marcus theory based result (27) to include the low-temperature limit, shows a characteristic behavior: electron-transfer induced

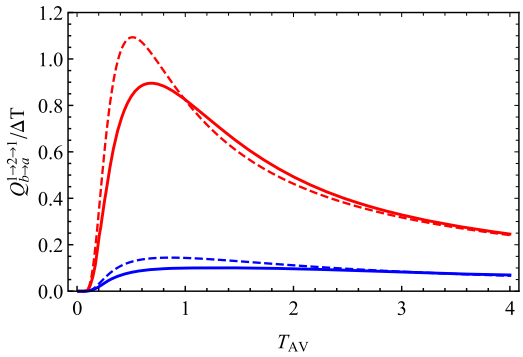

FIG. 3. The (scaled) heat transfer, $Q_{b\to a}^{1\to 2\to 1}/\Delta T$, into site a from site b for a round-trip process $1 \to 2 \to 1$, calculated by Eq. (29), plotted with respect to T_{AV}, for different values of E_{12} (0, dashed lines; 3, solid lines) and $E_{r_A} = E_{r_B} \equiv E_r$ (0.3, blue; 1.0, red). All parameters are in unit of ω_0.

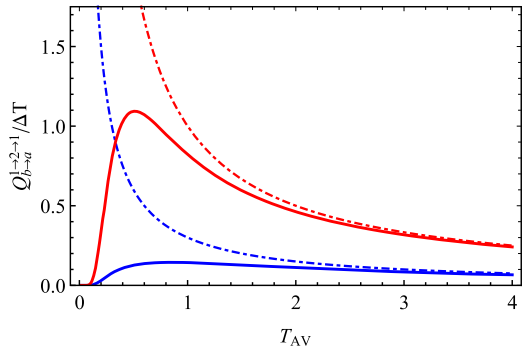

FIG. 4. The (scaled) heat transfer into site *a* over a round process, $Q_{b\to a}^{1\to2\to1}/\Delta T$, calculated from Eq. (27) (high temperature approximation, dotted-dashed lines) and Eq. (29) (general temperature, solid lines), respectively, with respect to T_{AV} on different reorganization energies $E_{r_a} = E_{r_b} \equiv E_r$ (0.3, blue; 1.0, red), and $E_{12} = 0$. All parameters are in unit of ω_0.

heat-transfer (ETIHT) vanishes in the limits $T \to 0$ and $T \to \infty$, going through a maximum in the intermediate temperature range, where $k_B T_{AV}$ is of order $\hbar\omega_0$. This is the main result of this paper.

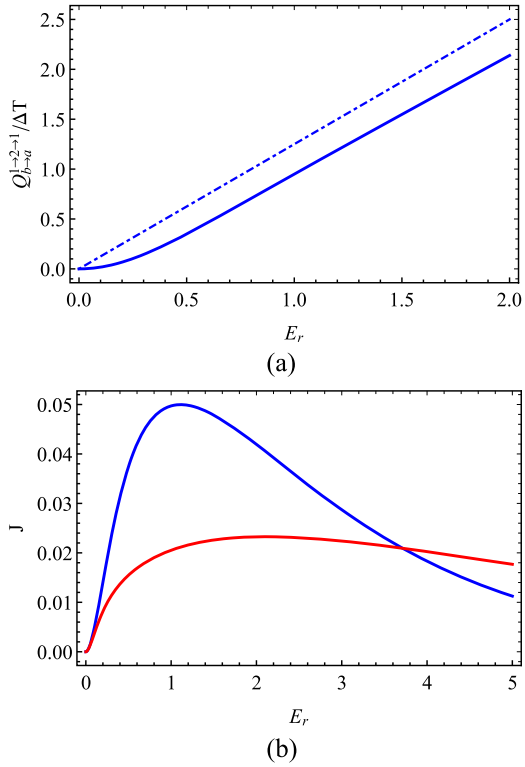

FIG. 5. Dependence on the reorganization energy: (a) the (scaled) heat transfer into site *a* over a round-trip process, $Q_{b\to a}^{1\to2\to1}/\Delta T$. The solid line is the full quantum calculation and the dashed-dotted line is the high temperature approximation; (b) the corresponding heat current, *J*, plotted against the reorganization energy, $E_{r_a} = E_{r_b} \equiv E_r$, of two identical sites. Parameters are in unit of ω_0: $\Delta T = 0.02$, $T_{AV} = 0.8$ (blue) or $T_{AV} = 2$ (red). Other parameters are as in Figs. 3 and 4.

(b) ETIHT is a manifestation of the electron-vibrational coupling, expressed in the present model by the reorganization energies of the modes involved. It is larger in systems exhibiting larger reorganization energies.

(c) In the high T_{AV} limit, the heat transfer does not depend on the difference ω_{12} between site energies. A modest dependence is seen at low temperatures. This weak dependence can be rationalized analytically, see the supplementary material, Sec. V.

(d) The amount of heat transferred per transferred electron increases with reorganization energy as shown in Figs. 3 and 4 as well as Fig. 5(a). Note that because the electron transfer rate itself vanishes in limits of zero and infinite reorganization energy, the heat flux, Eq. (24), goes through a maximum as a function of E_R, as shown in Fig. 5(b).[45]

IV. CONCLUSION

We have generalized our earlier theory of electron-transfer induced heat transfer (ETIHT) that was developed under the Marcus high-temperature approximation, to the low temperature regime, using a calculation based on the Fermi's golden rule approach. A proper accounting for the heat transfer depends critically on keeping a detailed balance property of the transfer rate exactly satisfied under any approximation used. Heat transfer accompanying electron transfer is a direct expression of the electron–phonon coupling in this system and increases with this coupling as expressed by the nuclear reorganization energies. The dependence of the energy difference between the electronic states involved is surprisingly manifested and vanishes in the high temperature limit.

As may be intuitively expected, as the average temperature approaches zero, the heat transfer induced by electron transfer vanishes, contrary to the divergence of the classical result. In this limit, the nuclear motion that accompanies electron transfer is essentially tunneling that does not rely on any excess nuclear energy. As a function of the average temperature, this contribution to heat transfer, therefore, goes through a maximum, which is realized near $k_B T = \hbar\omega$. This is the main new result of this paper.

The donor–acceptor model considered here provides a unified paradigm for the rate and extent of ET and heat transport, which can be generalized to systems with a variety of reaction pathways.[46,47] For example, it could be applied in a multiple geometrical arrangements to investigate the ET rate and heat transfer in planar geometries,[48–51] dielectric spheres,[52–55] photonic crystals,[56] microcavities,[57–60] etc. The enhancement or reduction in the thermoelectric effect in the performance of these systems would be further explored. On the theory side, the present calculation has disregarded the dynamics of the relaxation process that underlines the coupling of the vibrational modes that interact with the electronic subsystem to their thermal environment. Future work should examine this issue more closely.

SUPPLEMENTARY MATERIAL

See the supplementary material for the generalization of our treatment to many modes, the proof that detailed balance is satisfied by our result, and mathematical details in the derivation of Eqs. (23) and (29).

ACKNOWLEDGMENTS

This work was supported by the U.S. National Science Foundation under Grant No. CHE1953701. The authors thank Shahaf Nitzan for a helpful discussion that has contributed to Sec. III of the supplementary material.

AUTHOR DECLARATIONS

Conflict of Interest

The authors have no conflicts to disclose.

DATA AVAILABILITY

The data that support the findings of this study are available within the article and its supplementary material.

REFERENCES

[1]K.-H. Tang and R. E. Blankenship, "Photosynthetic electron transport," in *Encyclopedia of Biophysics*, edited by G. C. K. Roberts (Springer, Berlin, Heidelberg, 2013), pp. 1868–1873.
[2]W. Schmickler and J. Mohr, J. Chem. Phys. **117**, 2867 (2002).
[3]S. Kato, Microb. Biotechnol. **9**, 141 (2016).
[4]A. M. Oliveira-Brett, *Reference Module in Chemistry, Molecular Sciences and Chemical Engineering* (Elsevier, 2017).
[5]L. M. Peter, *Photocatalysis: Fundamentals and Perspectives* (The Royal Society of Chemistry, 2016), pp. 1–28.
[6]Y. W. Soon, T. M. Clarke, W. Zhang, T. Agostinelli, J. Kirkpatrick, C. Dyer-Smith, I. McCulloch, J. Nelson, and J. R. Durrant, Chem. Sci. **2**, 1111 (2011).
[7]A. P. Kulkarni, C. J. Tonzola, A. Babel, and S. A. Jenekhe, Chem. Mater. **16**, 4556 (2004).
[8]N. J. Tao, Nat. Nanotechnol. **1**, 173 (2006).
[9]R. A. Marcus, J. Chem. Phys. **24**, 966 (1956).
[10]R. A. Marcus and N. Sutin, Biochim. Biophys. Acta, Rev. Bioenerg. **811**, 265 (1985).
[11]N. R. Kestner, J. Logan, and J. Jortner, J. Phys. Chem. **78**, 2148 (1974).
[12]J. Ulstrup and J. Jortner, J. Chem. Phys. **63**, 4358 (1975).
[13]J. Jortner, J. Chem. Phys. **64**, 4860 (1976).
[14]J. Jortner and M. Bixon, J. Chem. Phys. **88**, 167 (1988).
[15]P. G. Wolynes, J. Chem. Phys. **87**, 6559 (1987).
[16]C. Zheng, J. A. McCammon, and P. G. Wolynes, Proc. Natl. Acad. Sci. U. S. A. **86**, 6441 (1989).
[17]C. Zheng, J. A. McCammon, and P. G. Wolynes, Chem. Phys. **158**, 261 (1991).
[18]J. S. Bader, R. A. Kuharski, and D. Chandler, J. Chem. Phys. **93**, 230 (1990).
[19]J. Cao, C. Minichino, and G. A. Voth, J. Chem. Phys. **103**, 1391 (1995).
[20]J. Cao and G. A. Voth, J. Chem. Phys. **106**, 1769 (1997).
[21]C. D. Schwieters and G. A. Voth, J. Chem. Phys. **108**, 1055 (1998).
[22]C. D. Schwieters and G. A. Voth, J. Chem. Phys. **111**, 2869 (1999).
[23]J. E. Lawrence and D. E. Manolopoulos, J. Chem. Phys. **153**, 154113 (2020).
[24]J. E. Lawrence and D. E. Manolopoulos, J. Chem. Phys. **153**, 154114 (2020).
[25]Z. Huang, B. Xu, Y. Chen, M. D. Ventra, and N. Tao, Nano Lett. **6**, 1240 (2006).
[26]M. Tsutsui, M. Taniguchi, and T. Kawai, Nano Lett. **8**, 3293 (2008).
[27]E. A. Hoffmann, H. A. Nilsson, J. E. Matthews, N. Nakpathomkun, A. I. Persson, L. Samuelson, and H. Linke, Nano Lett. **9**, 779 (2009).
[28]R. C. Maher, L. F. Cohen, E. C. Le Ru, and P. G. Etchegoin, Faraday Discuss. **132**, 77 (2006).
[29]Z. Ioffe, T. Shamai, A. Ophir, G. Noy, I. Yutsis, K. Kfir, O. Cheshnovsky, and Y. Selzer, Nat. Nanotechnol. **3**, 727 (2008).
[30]D. R. Ward, D. A. Corley, J. M. Tour, and D. Natelson, Nat. Nanotechnol. **6**, 33 (2010).
[31]N. C. Dang, C. A. Bolme, D. S. Moore, and S. D. McGrane, Phys. Rev. Lett. **107**, 043001 (2011).
[32]S. Sadat, A. Tan, Y. J. Chua, and P. Reddy, Nano Lett. **10**, 2613 (2010).
[33]F. Menges, H. Riel, A. Stemmer, and B. Gotsmann, Nano Lett. **12**, 596 (2012).
[34]W. Lee, K. Kim, W. Jeong, L. A. Zotti, F. Pauly, J. C. Cuevas, and P. Reddy, Nature **498**, 209 (2013).
[35]B. Desiatov, I. Goykhman, and U. Levy, Nano Lett. **14**, 648 (2014).
[36]Z. Chen, X. Shan, Y. Guan, S. Wang, J.-J. Zhu, and N. Tao, ACS Nano **9**, 11574 (2015).
[37]Y. Hu, L. Zeng, A. J. Minnich, M. S. Dresselhaus, and G. Chen, Nat. Nanotechnol. **10**, 701 (2015).
[38]M. Mecklenburg, W. A. Hubbard, E. R. White, R. Dhall, S. B. Cronin, S. Aloni, and B. C. Regan, Science **347**, 629 (2015).
[39]G. T. Craven and A. Nitzan, Proc. Natl. Acad. Sci. U. S. A. **113**, 9421 (2016).
[40]G. T. Craven and A. Nitzan, J. Chem. Phys. **146**, 092305 (2017).
[41]M. Bixon and J. Jortner, *Advances in Chemical Physics* (John Wiley & Sons, Inc., 2007), pp. 35–202.
[42]E. R. Heller and J. O. Richardson, J. Chem. Phys. **152**, 244117 (2020).
[43]A. Nitzan, *Chemical Dynamics in Condensed Phases*, Oxford Graduate Texts (Oxford University Press, Oxford, 2006).
[44]In the rate expression [Eq. (4)], $\widetilde{G}(\omega_{12})$ represents a process in which an amount of energy ω_{12} is given (when positive) to the vibrational space. The integral in Eq. (14) represents this as energy ω given to modes in site a and energy $\omega_{12} - \omega$ given to modes in site b, indicating that this contribution to the integral in Eq. (14) represents an amount ω of energy transfer between these sites.
[45]The limit $E_R \to 0$ should be handled with care: Expression (15) vanishes or diverges if the order in which we take the limits $E_{12} \to 0$ and $E_R \to 0$ interchanges. Physically a kinetic rate is not well defined in this limit, which corresponds to a model of coupled two-level system.
[46]G. T. Craven and A. Nitzan, Phys. Rev. Lett. **118**, 207201 (2017).
[47]V. Karanikolas, C. A. Marocico, and A. L. Bradley, Phys. Rev. A **89**, 063817 (2014).
[48]T. Kobayashi, Q. Zheng, and T. Sekiguchi, Phys. Lett. A **199**, 21 (1995).
[49]M. Cho and R. J. Silbey, Chem. Phys. Lett. **242**, 291 (1995).
[50]K. H. Drexhage, J. Lumin. **1–2**, 693 (1970).
[51]R. R. Chance, A. H. Miller, A. Prock, and R. Silbey, J. Chem. Phys. **63**, 1589 (1975).
[52]J. Gersten and A. Nitzan, J. Chem. Phys. **75**, 1139 (1981).
[53]J. I. Gersten and A. Nitzan, Chem. Phys. Lett. **104**, 31 (1984).
[54]L. M. Folan, S. Arnold, and S. D. Druger, Chem. Phys. Lett. **118**, 322 (1985).
[55]S. D. Druger, S. Arnold, and L. M. Folan, J. Chem. Phys. **87**, 2649 (1987).
[56]M. V. Erementchouk, L. I. Deych, H. Noh, H. Cao, and A. A. Lisyansky, J. Phys.: Condens. Matter **21**, 175401 (2009).
[57]G. S. Agarwal and S. D. Gupta, Phys. Rev. A **57**, 667 (1998).
[58]P. Andrew and W. L. Barnes, Science **290**, 785 (2000).
[59]D. M. Basko, F. Bassani, G. C. La Rocca, and V. M. Agranovich, Phys. Rev. B **62**, 15962 (2000).
[60]D. M. Basko, G. C. La Rocca, F. Bassani, and V. M. Agranovich, Phys. Status Solidi A **190**, 379 (2002).